BIOCHEMISTRY
including biophysical chemistry & molecular biology
Article

Biochemistry **2010,** *49,* 2715–2724 2715
DOI: 10.1021/bi9018658

Levodopa Deactivates Enzymes That Regulate Thiol−Disulfide Homeostasis and Promotes Neuronal Cell Death: Implications for Therapy of Parkinson's Disease[†]

Elizabeth A. Sabens,[‡] Anne M. Distler,[‡,∥] and John J. Mieyal*[,‡,§]

[‡]*Department of Pharmacology, Case Western Reserve University, School of Medicine, 2109 Adelbert Road, Cleveland, Ohio 44106-4965, and* [§]*Louis B. Stokes Veterans Affairs Medical Research Center, 10701 East Boulevard, Cleveland, Ohio 44106.* [∥]*Current address: Cuyahoga Community College, Cleveland, OH 44115.*

Received October 30, 2009; Revised Manuscript Received February 5, 2010

ABSTRACT: Parkinson's disease (PD), characterized by dopaminergic neuronal loss, is attributed to oxidative stress, diminished glutathione (GSH) levels, mitochondrial dysfunction, and protein aggregation. Treatment of PD involves chronic administration of Levodopa (L-DOPA) which is a pro-oxidant and may disrupt sulfhydryl homeostasis. The goal of these studies is to elucidate the effects of L-DOPA on thiol homeostasis in a model akin to PD, i.e., immortalized dopaminergic neurons (SHSY5Y cells) with diminished GSH content. These neurons exhibit hypersensitivity to L-DOPA-induced cell death, which is attributable to concomitant inhibition of the intracellular thiol disulfide oxidoreductase enzymes. Glutaredoxin (Grx) was deactivated in a dose-dependent fashion, but its content was unaffected. Glutathione disulfide (GSSG) reductase (GR) activity was not altered. Selective knockdown of Grx resulted in an increased level of apoptosis, documenting the role of the Grx system in neuronal survival. L-DOPA treatments also led to decreased activities of thioredoxin (Trx) and thioredoxin reductase (TR), concomitant with diminution of their cellular contents. Selective chemical inhibition of TR activity led to an increased level of apoptosis, documenting the Trx system's contribution to neuronal viability. To investigate the mechanism of inhibition at the molecular level, we treated the each isolated enzyme with oxidized L-DOPA. GR, Trx, and TR activities were little affected. However, Grx was inactivated in a time- and concentration-dependent fashion indicative of irreversible adduction of dopaquinone to its nucleophilic active-site Cys-22, consistent with the intracellular loss of Grx activity but not Grx protein content after L-DOPA treatment. Overall L-DOPA is shown to impair the collaborative contributions of the Grx and Trx systems to neuron survival.

Parkinson's disease (PD),[1] the second most common neurodegenerative disease, is characterized by bradykinesia, resting tremor, rigidity, and postural instability. PD affects mostly catecholaminergic neurons in the *substantia nigra* of the brain (*1*), and it is linked to both genetic and environmental factors, involving oxidative stress, mitochondrial dysfunction, and protein aggregation (*2*). Many reports have attributed the pathogenesis of PD to the oxidative stress concomitant with an increased rate of dopamine turnover, deficient glutathione content, and an increased iron level in the *substantia nigra* (*3*).

The primary agent for current therapy of PD is L-DOPA, a precursor of dopamine, serving to restore dopaminergic signals from catecholaminergic neurons. Typically, L-DOPA is used at increasing doses as the disease progresses. Furthermore, L-DOPA treatment of rodents is reported to increase the level of lipid peroxidation, characteristic of oxidative stress (*3*). Exposing cultured pheochromocytoma cells (PC12 cells) to increasing concentrations of L-DOPA has led to cell detachment resulting in cell death (*4*). These outcomes are attributed to the metabolism of L-DOPA creating reactive oxygen species (ROS), superoxide, and hydrogen peroxide which could promote both reversible (disulfide and sulfenic acid) and irreversible (sulfinic and sulfonic acids) modifications of protein cysteine (Cys) residues (Scheme 1). Furthermore, highly reactive quinone species can be formed from L-DOPA and its products, dopamine and DOPAC, which may react with exposed Cys residues on proteins (Scheme 1).

Studies performed with isolated L-DOPA show spontaneous and nonenzymatic oxidation to ROS and reactive quinones (*5*). Such reactive quinone species can irreversibly conjugate to Cys residues on proteins, forming S-cysteinyl dopamine adducts, thereby altering protein function (*2*). Moreover, there is evidence that this may occur in PD patients. Thus, post-mortem human brain tissue samples from L-DOPA-treated versus control showed a significant increase in the level of quinone adducts, with the highest quantities found within the *substantia nigra* (*6*). A recent review of clinical trials focused on potential L-DOPA

[†]This work was supported in part by National Institutes of Health (NIH) Grant PO1 AG 15885 (J.J.M.), a Department of Veterans Affairs Merit Review Grant (J.J.M.), and NIH Training Grants T32 GM008803 and T32 DK007319 (E.A.S.).

*To whom correspondence should be addressed. Telephone: (216) 368-3383. Fax: (216) 368-8887. E-mail: jjm5@cwru.edu.

[1]Abbreviations: ATCC, American Type Culture Collection; BSA, bovine serum albumin; BSO, buthionine sulfoximine; CSSG, cysteinyl-S-S-glutathione mixed disulfide; DA, dopamine; DOPAC, 3,4-dihydroxyphenylacetic acid; DTNB, 5′,5-dithiobis(2-nitrobenzoic acid) (Ellman's reagent); EDTA, ethylenediaminetetraacetic acid; GR, glutathione disulfide reductase; Grx, glutaredoxin; GSH, glutathione; GSSG, glutathione disulfide; HEDS, hydroxyethyl disulfide; 6-OHDA, 6-hydroxydopamine; L-DOPA or Levodopa, L-3,4-dihydroxyphenylalanine; MPP+, 1-methyl-4-phenylpyridinium; MPTP, 1-methyl-4-phenyl-1,2,3,6-tetrahydropyridine; MTT, (4,5-dimethylthiazol-2-yl)-2,5-diphenyltetrazolium bromide; NADPH, nicotinamide adenine dinucleotide phosphate; PD, Parkinson's disease; Trx, thioredoxin; TR, thioredoxin reductase.

Published on Web 02/08/2010

Scheme 1: (A) Selective Activities of the Thioredoxin (Trx) and Glutaredoxin (Grx) Systems[a] and (B) Pro-Oxidant Metabolism of L-DOPA[b]

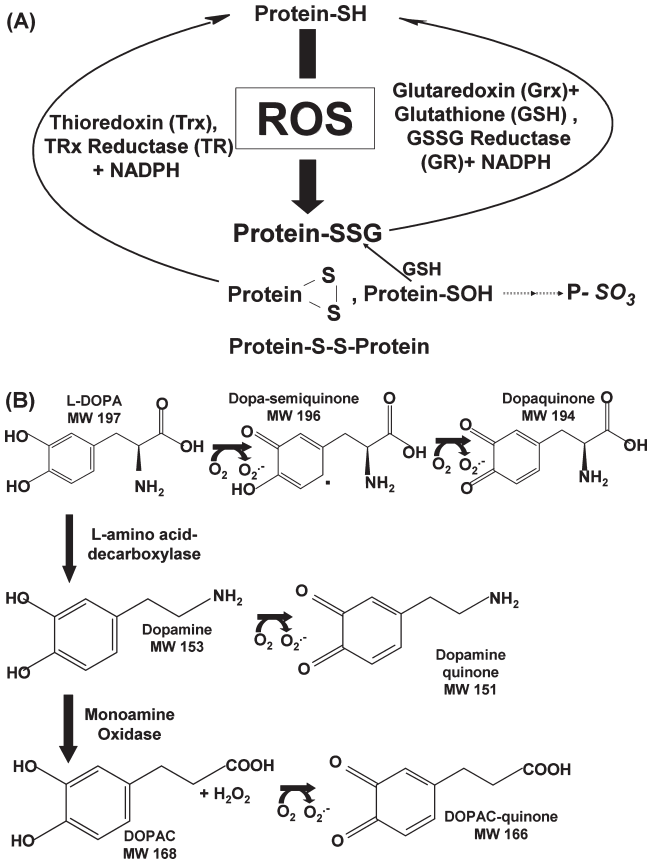

[a]Grx selectively reduces glutathionylated proteins (Protein-SSG), whereas Trx is able to reduce intermolecular disulfides (Protein-SS-Protein) and intramolecular disulfides. [b]L-DOPA is oxidized to semiquinone and quinone forms, releasing superoxide. Also, L-DOPA undergoes a decarboxylation reaction by L-amino acid decarboxylase to form dopamine. Dopamine can undergo similar oxidations to L-DOPA, forming both semiquinone and quinone species. Formation of these oxidized products results in the release of superoxide. Lastly, dopamine is degraded by monoamine oxidase, forming 3,4-dihydroxyphenylacetic acid (DOPAC). Formation of this degradation product releases superoxide. Also, DOPAC can similarly form the reactive quinone species as shown in the bottom of panel B.

toxicity in patients portrayed an ambiguous picture and suggested further clinical and basic science studies are necessary to advance our understanding (*7*).

In this study, biochemical and molecular mechanisms underlying the potential consequences of L-DOPA therapy were explored using a PD cell culture model, SHSY5Y immortalized dopaminergic neurons. These cells exhibit dopaminergic characteristics, including expression of tyrosine hydroxylase and production of dopamine and its metabolites (*8*, *9*). Since L-DOPA metabolism can promote thiol oxidation (*5*) and thiol homeostasis is important for cell survival, we investigated L-DOPA-induced apoptosis and focused on alterations in thiol homeostatic enzymes within SHSY5Y neurons.

Here we report that L-DOPA treatment of SHSY5Y neurons leads to apoptotic cell death. Concomitantly, Grx is deactivated without a change in its cellular content. Furthermore, there are partial losses of TR and Trx activities upon L-DOPA treatment, with corresponding losses in their contents, suggesting a different mechanism of deactivation. Biochemical studies of the isolated enzymes showed only Grx, and not GR, Trx, or TR, is inactivated substantially when exposed to oxidized L-DOPA, leading to a specific active-site adduct. Selective knockdown of Grx or selective chemical inhibition of TR each led to an increased level of apoptosis. These model studies suggest that alteration of thiol homeostasis through deactivation of key enzymes contributes to the overall loss of dopaminergic neurons in PD patients.

MATERIALS AND METHODS

Materials. Cysteinyl-glutathione mixed disulfide was purchased from Toronto Research Chemicals. NADPH was purchased from Roche. TR, GR, and Trx were purchased from Sigma. Plasmid DNA (pET-24d, Novagen) encoding human Grx1 was prepared as described by Chrestensen et al. (*10*). siRNA SMARTpool was purchased from Dharmacon. Hoechst 33342 trihydrochloride and cell culturing supplies were purchased from Invitrogen. All other reagent grade chemicals were purchased from Sigma.

Synthesis of [^{3}H]BSA-SS-Glutathione Mixed Disulfide Substrate. This radiolabeled prototype substrate for Grx was prepared as described previously (*11*), except that [^{3}H]GSH was substituted for [^{35}S]GSH in the formation of the final product. [^{3}H]BSA-SSG was isolated by gel filtration, and its specific radioactivity corresponded to a 1:1 stoichiometry of glutathionyl moiety and BSA protein.

Cell Culture. SHSY5Y cells were obtained from the ATCC. Cells were maintained under an atmosphere of air and 5% CO_2 at 37 °C. The medium was comprised of a 1:1 mixture of MEM and Hams F12 medium (Mediatech, Cell Gro), containing 0.01 mM sodium pyruvate, 1 μM nonessential amino acids, and 10% certified fetal bovine serum. Cells were plated in 96-well plates (MTT assay), six-well plates (Hoechst staining), or 100 mm dishes and allowed to come to ~75% confluency prior to treatment.

Treatments of Cells in Culture. L-DOPA was added to cell culture media for 24 h at concentrations ranging from 0 to 1 mM.

Treatment with 0.1 mM BSO (buthionine sulfoximine) for 24 h resulted in approximately 80% diminution of the GSH level, within the range of GSH loss in PD patients. This concentration of BSO (added concurrently with L-DOPA) was used for the experiments reported in Results.

Auranofin was added to culture media at various concentrations for 30 min. After 30 min, the medium was changed and cells were either harvested immediately for measurements of TR activity or maintained for 24 h for measurements of chromatin condensation by Hoechst staining.

Isolation and Purification of Grx. Grx was overexpressed in *Escherichia coli* via a plasmid DNA construct and purified to homogeneity (specific activity of ~100 units/mg) as described by Jao et al. (*12*).

Treatment of Purified Thiol Disulfide Oxidoreductase Enzymes with Oxidized L-DOPA. L-DOPA was dissolved in 1× phosphate buffered saline (1×PBS) and allowed to oxidize overnight while exposed to air at 37 °C (*5*). Enzyme was incubated with various concentrations of L-DOPA or 1×PBS (control) at 30 °C over the course of 1 h. At various time points, aliquots of enzyme were removed and their respective activities assayed (see below). Inhibition was measured as a percentage of activity lost compared to the control.

Grx Activity. Our standard spectrophotometric coupled enzymatic assay was performed as described in ref *13*. Grx activity (formation of GSSG from CSSG), corresponding to

micromoles of NADPH oxidized per minute, was calculated using the extinction coefficient for NADPH (ε = 6.2 mM^{-1} cm^{-1}), along with correction factors to normalize plate reader values to standard spectrophotometer readings (*11*).

Trx Activity. A spectrophotometric coupled enzymatic assay was performed as described in ref *14*. Reaction mixtures containing Na/K phosphate buffer (0.1 mM, pH 7.5), NADPH (0.2 mM), thioredoxin reductase (TR) (0.09 unit), and Trx (0.24 unit) were prepared in individual wells of a 96-well plate in a final volume of 200 μL and incubated for 5 min at 30 °C. Care was taken to ensure that TR, as the coupling enzyme, was not limiting. Reactions were initiated with the addition of 2 mM HEDS, and NADPH oxidation, corresponding to reduction of Trx-S_2, was monitored at 340 nm for 5 min. Units of Trx activity were calculated in a manner analogous to that used for Grx activity (above).

Thioredoxin Reductase Activity. TR activity was measured by observation of NADPH-dependent reduction of 5,5′-dithiobis(2-nitrobenzoic acid) (DTNB) as adapted from a Sigma protocol. Briefly, NADPH (0.24 mM), DTNB (5 mM), BSA (0.2 mg/mL), and EDTA (10 mM) were combined in 100 mM Na/K phosphate buffer (pH 7.0) (final volume of 600 μL). TR was added to initiate the reaction which was monitored at A_{412} for 1 min. Activity was calculated in "DTNB units", i.e., ΔA_{412} per minute (volume of assay per enzyme volume).

Glutathione Disulfide Reductase Activity. GR activity was measured spectrophotometrically, using an assay adapted from ref *15*. K phosphate buffer (0.1 M), EDTA (1 mM, pH 7.0), NADPH (0.1 mM), and GSSG (final concentration of 1 mM) were incubated for 5 min at room temperature. GR was added to initiate the reaction (5.5 milliunits), and the change in absorbance at 340 nm was monitored for 5 min. Enzymatic activity was calculated in a manner analogous to that used for Grx activity.

Cell Viability. Cell viability was measured according to the reactivity of MTT [3-(4,5-dimethylthiazol-2-yl)-2,5-diphenyltetrazolium bromide]. The MTT solution (final concentration of 0.5 mg/mL) was placed on the cells for 2 h at 37 °C. Then an equal volume of MTT solubilization solution (0.1 N HCl with anhydrous 2-propanol and 10% Triton X) was added with shaking at room temperature for 1 h to solubilize the formazan crystals. The absorbance reading at 570 nm for each well was recorded, and the corresponding nonspecific absorbance at 690 nm was subtracted according to the manufacturer's protocol.

Cell Death Measurements. Trypan blue exclusion was used to assess overall cell death. Trypan blue dye was mixed with an equal volume of cells. Those cells that took up the dye and turned blue were counted as dead. Hoechst 33342 trihydrochloride, used to analyze chromatin condensation indicative of apoptosis, was added to medium (final concentration of 10 μM) for 10 min at 37 °C. Cells were counted on a Leica microscope with a DAPI fluorescence filter. Quantitative analysis of Hoechst staining of the cells was conducted in a blinded fashion relative to the respective treatments.

Grx Activity in Cell Lysates. Cells were collected in NP40 lysis buffer without protease inhibitors. The resulting cell lysates were analyzed immediately for GSH-dependent deglutathionylation of [^{3}H]BSA-SSG as described previously (*11*).

Trx and TR Activity in Cell Lysates. Trx activity and TR activity were measured according to reduction of insulin disulfides and detection of the thiols by DTNB, as described by Arner et al. (*16*). SHSY5Y cells were ruptured in a lysis buffer comprised of 100 mM NaCl, 20 mM Tris (pH 8), 0.5 mM EDTA, 0.5% (v/v) NP-40, 1 mM sodium orthovanadate, 10 mM sodium pyrophosphate, and 20 mM sodium fluoride; 30 μg of cell lysate (protein content) was incubated in a final volume of 50 μL containing 0.3 mM insulin, 0.66 mM NADPH, 2.5 mM EDTA, and 27 milliunits of TR or 0.24 unit of Trx (depending on which enzyme was being assayed as the limiting factor) in 85 mM HEPES (pH 7.6) for 40 min at 37 °C. After incubation at 37 °C, the reaction was stopped by the addition of 200 μL of 8 M guanidine hydrochloride containing 1 mM DTNB, and the absorbance at 405 nm was read immediately. Separate experiments confirmed that these conditions were within the linear range of the time and concentration dependence of the corresponding enzyme activities. Control measurements were taken for each sample of cell lysate in the absence of additional enzyme. The control DTNB reactivity, corresponding to free thiols in the cell, was subtracted from values for lysates containing exogenous enzyme. Background absorbance, likely due to cellular thiols in the lysate, was subtracted, and the net change in A_{405} at 40 min was converted to specific enzyme activity (micromoles of thiol per minute per milligram) according to a standard curve for thiol (GSH) content generated under the same conditions.

GR Activity in Cell Lysates. Cell lysates (20−40 μg) were added to a reaction mixture comprised of 0.1 M K phosphate and 0.1 mM EDTA (pH 7.0) (final concentration); 2 mM NADPH dissolved in 10 mM Tris-HCl (pH 7.0) was added to buffer to give a final concentration of 0.1 mM. Reaction mixtures were incubated for 5 min at 37 °C. Reactions were initiated by the addition of GSSG (final concentration of 1 mM). Loss of NADPH absorbance (340 nm) was read continuously for 5 min to produce the GR-mediated rate (*14*).

Western Blotting. To determine the relative content of specific proteins, 100 μg (total protein) of lysate was loaded on SDS−PAGE gels (12.5%) and separated. Proteins were transferred to polyvinylidene fluoride (PVDF) membranes (Millipore Corp.). Samples were probed with either Grx1 (1:1000), generated via adaptation of the caprylic acid method of McKinney and Parkinson (*17*), Trx1 (5 μg/mL), polyclonal sheep anti-human antibody (Quality Control Biochemicals) generated from peptide sequences of Trx1 protein, or TR1 (1:1000, Santa Cruz), and the relative content was determined by densitometric analysis (Quantity One, Bio-Rad) compared to the loading control, actin (1:30000) (Sigma).

Knockdown of Grx. SHSY5Y cells were treated with lipofectamine 2000 and SMARTpool siRNA directed to specific sequences of human Grx mRNA (Dharmacon). Knockdown was performed according to the manufacturer's protocol (Invitrogen). Lipofectamine 2000 and 140 nM siRNA (final concentration) were used to give ~50% knockdown of Grx. Control experiments involved transfection with scrambled siRNA sequences. Transfections were stopped 12 h after initiation, and cells were harvested 48 h after transfection.

Adduction of Grx by Oxidized L*-DOPA and Mass Spectrometry*. Purified Grx (100 μg) was incubated with oxidized L-DOPA or buffer for 1 h. Inactivation of the enzyme was confirmed by the spectrophotometric assay. Grx samples were purified with C-18 ZipTips (Millipore) according to the manufacturer's instructions, the exception being that the samples were eluted with a larger volume of elution solution (50 μL). The samples were infused directly into the Applied Biosystems Q-STAR XL mass spectrometer in positive ion mode. For intact protein analysis, the mass spectra were deconvoluted using BioAnalyst. Trypsin (20 μg/mL in 25 mM ammonium

bicarbonate) was used to digest Grx. Grx samples (treated with oxidized L-DOPA and untreated) were incubated with trypsin (1:25 trypsin:protein ratio) for 4 h at 37 °C. The MS/MS spectra were analyzed using MASCOT, and assignments were confirmed by manual inspection.

RESULTS

Diminution of the GSH Concentration in SHSY5Y Cells Leads to Increased Sensitivity to L-DOPA. In Parkinson's disease brains, the *substantia nigra* has a decreased antioxidant capacity mainly due to the diminution of GSH levels (*18*−*20*). To examine whether diminution of GSH leads to increased sensitivity to the oxidative insult associated with L-DOPA treatment, we decreased the GSH content with BSO (0.1 mM): ~80% GSH depletion at 24 h in immortalized dopaminergic neurons (SHSY5Y cells) (control, 0.68 ± 0.06 mM; BSO-treated, 0.13 ± 0.01 mM). A similar loss of GSH is seen with PD (*18*).

To assess cell sensitivity to L-DOPA, several assays of cell death were performed. Treatment of SHSY5Y cells for 24 h with L-DOPA led to a dose-dependent decrease in cell viability according to the loss of MTT reactivity, and the dose−response curve was shifted to the left in cells that were cotreated with 0.1 mM BSO (Figure 1A). The dose−response relationship for the L-DOPA-dependent increase in the level of cell death (trypan blue analysis) was also shifted to lower concentrations in GSH-deficient cells (Figure 1B). The level of apoptosis (according to chromatin condensation) increased with an increasing L-DOPA level, occurring at lower concentrations with BSO cotreatment. The majority of cell death is attributed to apoptosis since quantification of cells positive for chromatin condensation (Hoechst staining) corresponded closely to the extent of cell death assessed with trypan blue (Figure 1C). Sensitivity to L-DOPA cytotoxicity was increased approximately 3-fold, according to all assays, when GSH was depleted by cotreatment with BSO.

Having documented L-DOPA dose-dependent cell death with SHSY5Y neurons, we wanted to examine potential mechanisms involving perturbation of sulfhydryl homeostasis. Metabolism of L-DOPA can generate ROS and reactive quinones (Scheme 1), all of which can lead to protein-SH modifications. The greatest impact of such reactivity would be realized if the homeostatic enzymes themselves (Scheme 1) were modified by L-DOPA byproducts. The two principal enzyme systems that mediate sulfhydryl homeostasis within cells are thioredoxin (Trx) and glutaredoxin (Grx), which catalyze the reduction of oxidized cysteine moieties (*21*−*23*). Thioredoxin effectively reduces intramolecular and intermolecular disulfides as well as sulfenic acids (*24*). Glutaredoxin specifically reduces protein-glutathione mixed disulfides (protein-SSG) (*22*). The different specificities suggest that the Trx and Grx systems act synergistically to maintain cellular sulfhydryl homeostasis. Therefore, we investigated how L-DOPA treatment affected the activities of these enzymes.

Thiol Disulfide Oxidoreductase Enzymes Are Differentially Affected by L-DOPA Treatment. In other contexts, Grx has been reported to be altered under oxidative stress conditions, resulting in changes in activity and/or content (reviewed in ref *25*). Therefore, we examined how L-DOPA affected both Grx content and activity. L-DOPA, even at the highest concentration used, did not decrease Grx content (Figure 2A,B). In contrast, Grx activity was diminished in a dose-dependent fashion with increasing concentrations of L-DOPA (Figure 2C). Cotreatment with BSO led to an increased sensitivity of Grx to

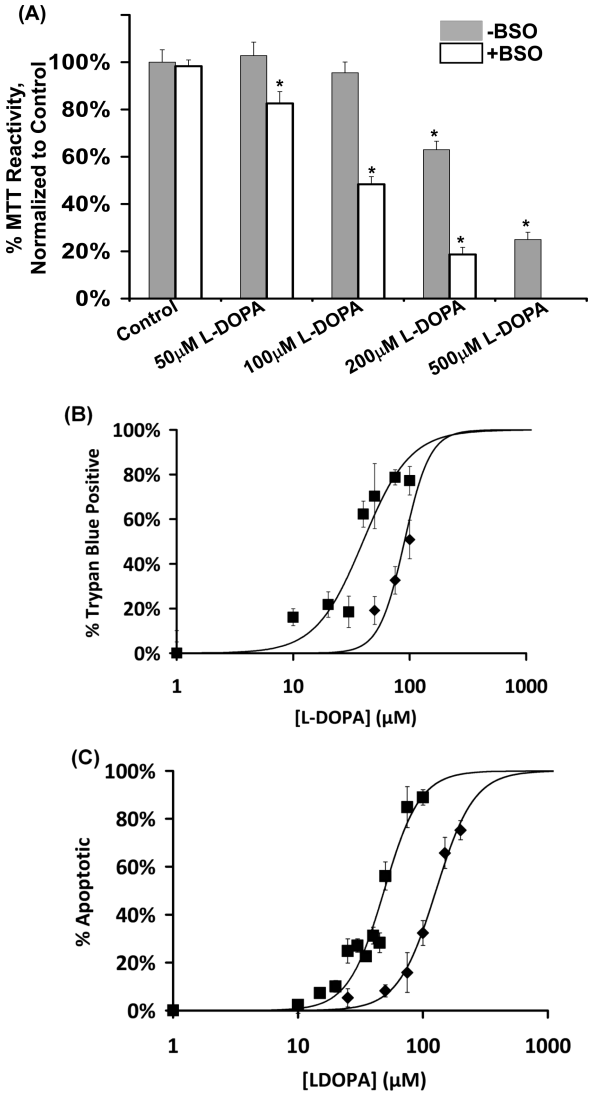

FIGURE 1: Diminution of GSH concentration in SHSY5Y cells leads to increased sensitivity to L-DOPA and an increased level of cell death. (A) Bar graph displaying relative cell viability as measured by the MTT assay (see Materials and Methods) when treated with L-DOPA for 24 h. Solid bars represent data for cells with replete GSH. Empty bars indicate data for cells treated with 0.1 mM BSO. BSO treatment showed a 3-fold increase in sensitivity to L-DOPA. Asterisks denote significant differences compared to control ($p < 0.01$; $n = 3$). (B) Dose−response curves for L-DOPA-dependent cell death (trypan blue). SHSY5Y cells were treated with L-DOPA for 24 h, and trypan blue was used to measure cell death, as described in Materials and Methods. Treatment in the presence of BSO led to ~3-fold sensitization of SHSY5Y cells to L-DOPA-induced cell death: (■) BSO- and L-DOPA-treated cells and (◆) samples treated with only L-DOPA. (C) Dose−response curves for L-DOPA-dependent apoptosis (Hoechst staining). SHSY5Y cells were treated with L-DOPA for 24 h, and the level of apoptosis was measured using Hoechst 33342, determining the extent of chromatin condensation (see Materials and Methods). Samples were counted in triplicate in a blinded fashion: (■) BSO- and L-DOPA-treated cells and (◆) samples treated with only L-DOPA. The curves in Figure 1 were fit to the percent apoptosis vs L-DOPA concentration data according to the following equation, minimizing the least-squares deviation: percent apoptosis = $\text{effect}_{max}[\text{L-DOPA}]^n/(EC_{50})^n + [\text{L-DOPA}]^n$, where n is equivalent to the Hill coefficient. The EC_{50} values for L-DOPA-induced apoptosis calculated from the fitted curves are 49 μM (with BSO) and 127 μM (without BSO).

inhibition by L-DOPA treatment, as shown in Figure 2C, by more than 2-fold. In contrast to Grx, the coupling enzyme for the Grx system, GR, was essentially insensitive to L-DOPA. Figure 3A

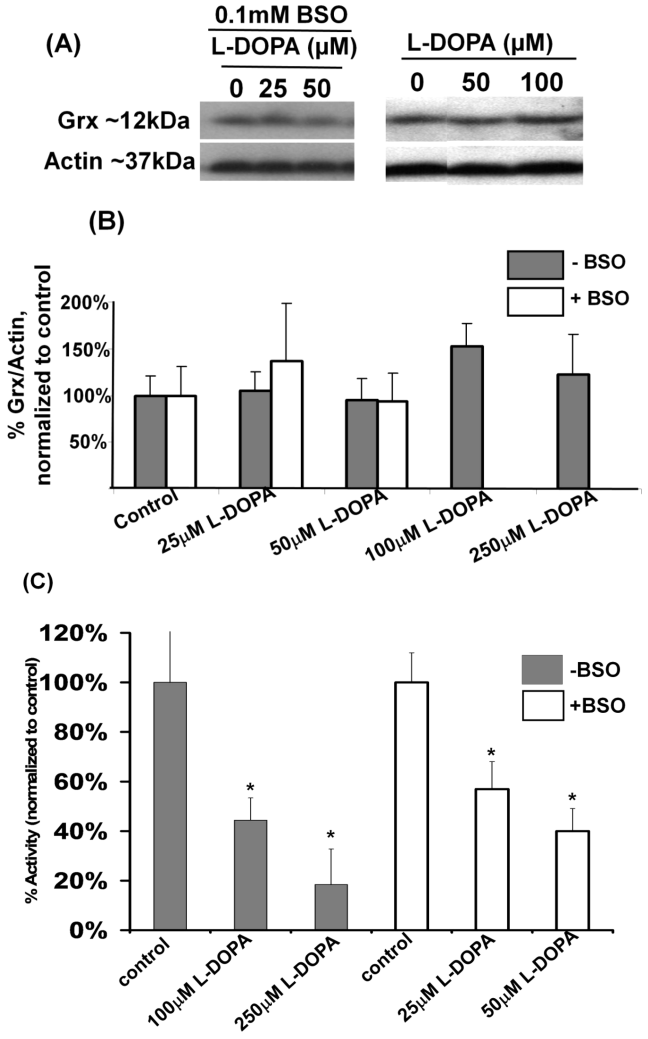

FIGURE 2: Grx is deactivated within SHSY5Y cells upon L-DOPA treatment. (A) Typical Western blot showing Grx content in lysates of SHSY5Y cells, relative to actin (loading control). (B) Bar graph displaying densitometric quantification of Western blots for Grx content in SHSY5Y cells under various conditions. Solid bars represent data for cells with replete GSH. Empty bars indicate data for cells treated with 0.1 mM BSO. No statistically significant change in Grx content is evident ($n = 3$; $p > 0.5$) for most comparisons. The content value for 100 μM L-DOPA treatment tends toward an anomalous but insignificant increase in Grx content ($n = 8$; $p = 0.17$). (C) Bar graph displaying Grx activity assayed according to the release of radiolabel ([^{3}H]GSSG) from the prototypical substrate, [^{3}H]BSA-SSG. Solid bars represent data for cells with replete GSH. Empty bars indicate data for cells treated with 0.1 mM BSO. The Grx activity for the control is 0.854 ± 0.21 nmol min^{-1} (mg of protein)$^{-1}$; the Grx activity for the BSO-treated control is 0.703 ± 0.188 nmol min^{-1} (mg of protein)$^{-1}$. BSO provided an ~2-fold increase in the loss of Grx activity. Asterisks denote significant differences compared to control ($p < 0.01$; $n \geq 3$).

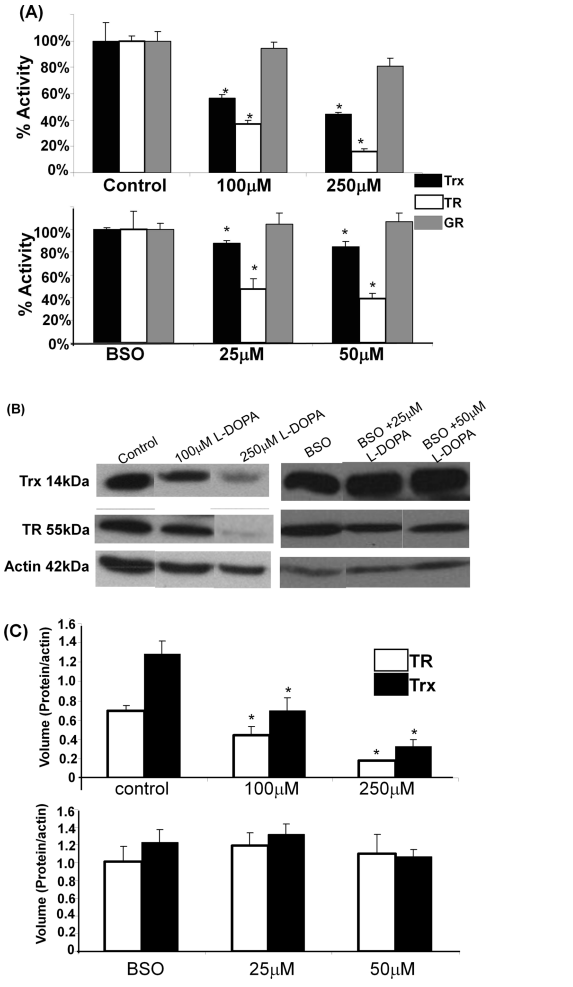

FIGURE 3: GR activity is not affected by L-DOPA treatment; however, the levels of the thioredoxin system proteins, TR and Trx, are diminished upon L-DOPA treatment. (A) Bar graph of relative activities. Activities of the respective enzymes were measured as described in Materials and Methods for SHSY5Y cells treated with L-DOPA, either in the absence of BSO (replete GSH, top panel) or in the presence of 0.1 mM BSO (decreased GSH, bottom panel). Black bars represent Trx activity, white bars TR activity, and gray bars GR activity. In the top panel (replete GSH), the Trx activity (black bars) showed significant L-DOPA concentration-dependent decreases [asterisks indicate $p < 0.05$ ($n = 3$)]. The Trx activity measured for the control is 1.76 ± 0.04 units/mg of protein. TR activity (white bars) showed significant L-DOPA concentration-dependent decreases [asterisks indicate $p < 0.05$ ($n = 3$)]. The TR activity measured for the control is 1.98 ± 0.32 units/mg of protein. The GR activity (gray bars) was not significantly changed. The GR activity for the control is 2.2 ± 0.3 units/mg of protein. In the bottom panel (diminished GSH), the Trx activity (black bars) showed small but significant L-DOPA concentration-dependent decreases [asterisks indicate $p < 0.05$ ($n = 3$)]. The Trx activity for the control is 1.91 ± 0.26 units/mg of protein. Decreases in TR activity (white bars) indicated a 5-fold increased sensitivity to L-DOPA when the GSH concentration was diminished. The TR activity for the control is 1.92 ± 0.07 units/mg of protein. The GR activity (gray bars) was not significantly changed. The GR activity for the control is 1.81 ± 0.19 units/mg of total protein. (B) Typical Western blot showing TR and Trx reactivity relative to actin (loading control). (C) Bar graph of relative contents. Densitometric quantification of TR and Trx content using QuantityOne. All samples were normalized to actin, the loading control. Asterisks indicate $p < 0.05$ ($n = 3$).

shows the enzymatic activity of GR is essentially unaffected by concentrations of L-DOPA of ≤ 100 μM, and $< 20\%$ inhibited at 250 μM L-DOPA.

With the Trx system, the activities of TR and Trx were decreased in an L-DOPA-dependent manner (Figure 3A). Unlike Grx, in cells with replete GSH content, the loss of TR and Trx activities corresponded to proportional losses in the content of the respective proteins as documented by Western blot analysis (Figure 3B,C). Furthermore, Trx did not display increased sensitivity to BSO treatment, showing little inhibition ($< 20\%$). Unlike Trx and similar to Grx, TR was more sensitive (~3−4-fold) to inhibition from L-DOPA treatment in the GSH-depleted cells (BSO-treated), and in this case, the TR content did not change. These findings suggest a shift in the mechanism of inhibition of the Trx system when GSH is depleted (see Discussion).

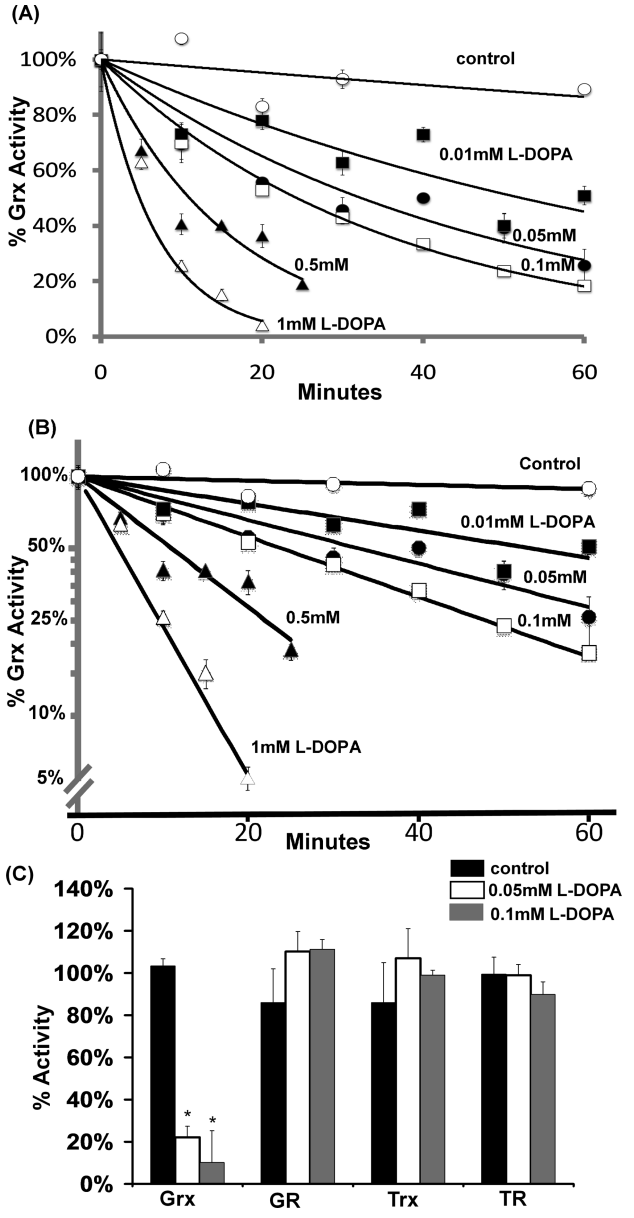

FIGURE 4: Grx is the only thiol disulfide oxidoreductase inactivated by oxidized L-DOPA. (A) Isolated Grx was incubated with L-DOPA, and aliquots of the reaction mixture were withdrawn every 10 min and assayed for enzyme activity as described in Materials and Methods. The Grx activity was decreased in a time- and dose-dependent fashion. (B) Semilog plot of the data shown in panel (A). Straight lines with increasing negative slopes are indicative of pseudo-first-order enzyme inactivation. (C) Each isolated enzyme was incubated in the absence or presence of oxidized L-DOPA, and aliquots of the reaction mixture were withdrawn every 20 min and assayed for the respective enzyme activities as described in Materials and Methods. GR, Trx, and TR activities were unaffected, even when tested in separate experiments where the aliquots were withdrawn at 60 min intervals. Grx was inactivated in an oxidized L-DOPA-dependent manner; asterisks denote significant differences relative to the control ($p < 0.015$; $n = 3$).

Oxidized L-DOPA Grx Selectively Inactivates Grx in Vitro. As described above, quinone adduction is a potential mechanism by which L-DOPA treatment may lead to inhibition of the thiol disulfide oxidoreductases. Therefore, we studied time- and concentration-dependent inactivation of the purified enzymes by oxidized L-DOPA. Grx was inactivated in a dose-dependent fashion according to pseudo-first-order kinetics (Figure 4A,B). Addition of GSH to the preincubation mixture protected Grx, consistent with data from cells with replete GSH (Figure 2C). Inactivation of Grx by quinone adduction would be expected to involve the active-site Cys-22, which possesses a unique thiol pK_a of 3.5 (see below).

The other thiol disulfide oxidoreductases were tested with oxidized L-DOPA in an analogous fashion. GR, Trx, and TR exhibited very little sensitivity to oxidized L-DOPA (Figure 4C). While most of the effects on enzyme activities in the cell studies are consistent with the observations with the isolated enzymes, the lack of adductive inactivation of the isolated TR contrasts remarkably with the loss of TR activity without a loss of TR protein in GSH-deficient cells treated with L-DOPA (see Discussion).

Dopaquinone Adducts to Grx at the Active Site. To determine the site(s) of covalent quinone modification resulting in Grx inactivation, purified Grx protein was treated with oxidized L-DOPA and then analyzed by mass spectrometry. After inactivation of the Grx, we observed an increase of 194 mass units in the deconvoluted mass spectrum (Figure 5A). This is indicative of adduction of one dopaquinone to Grx. Upon trypsin digestion of the protein and fragmentation of the tryptic peptides using MS/MS, the adduction at the active site was confirmed. A mass shift of m/z 194 was detected at Cys-22 when the untreated protein (Figure 5B) was compared to the inactivated protein (Figure 5C). Modification at this site is consistent with inactivation because Cys-22 is required for the catalytic activity of Grx1. Despite the overabundance of oxidized L-DOPA, only Cys-22 was adducted by dopaquinone.

Grx Knockdown in SHSY5Y Cells Leads to Apoptosis. Although a loss of Grx activity is apparent, other events may contribute to L-DOPA-dependent increases in the level of apoptosis. Therefore, we tested whether selective loss of Grx activity would result in an increased level of apoptosis by using siRNA directed against Grx1 production in SHSY5Y cells. The extent of knockdown of Grx1 was confirmed by Western blot (Figure 6A). We chose to knock down Grx1 by 50% to approximate the amount of residual active Grx observed with 100 μM L-DOPA treatment of the cells (Figure 3C). Knockdown of Grx1 by ~50% led to an ~30% increase in the level of apoptosis, as measured by nuclear chromatin condensation compared to cells transfected with scrambled siRNA or mock transfected cells (Figure 6B). A 30% increase in the level of apoptosis accounts for most of the apoptosis observed with 100 μM L-DOPA treatment under conditions of replete GSH. This result further implicates Grx as an important regulator of cell death within SHSY5Y cells.

Auranofin-Induced Inhibition of TR Leads to Apoptosis. To inhibit TR selectively, we used the well-characterized chemical inhibitor auranofin (*26*, *27*) and titrated its concentration to inhibit TR to a an extent similar to that seen with BSO and L-DOPA treatment of the cells. Treatment of SHSY5Y cells with auranofin led to an increased level of apoptosis in a dose-dependent fashion (Figure 7A), in parallel with an increasing level of inhibition of TR (Figure 7B). These results support the conclusion that TR activity also is important for cell survival in SHSY5Y cells.

DISCUSSION

In this study, we investigated potential mechanisms by which L-DOPA treatment alters thiol homeostasis leading to cell death in immortalized neurons. It is noteworthy that the range of concentrations of L-DOPA that are neurotoxic in the

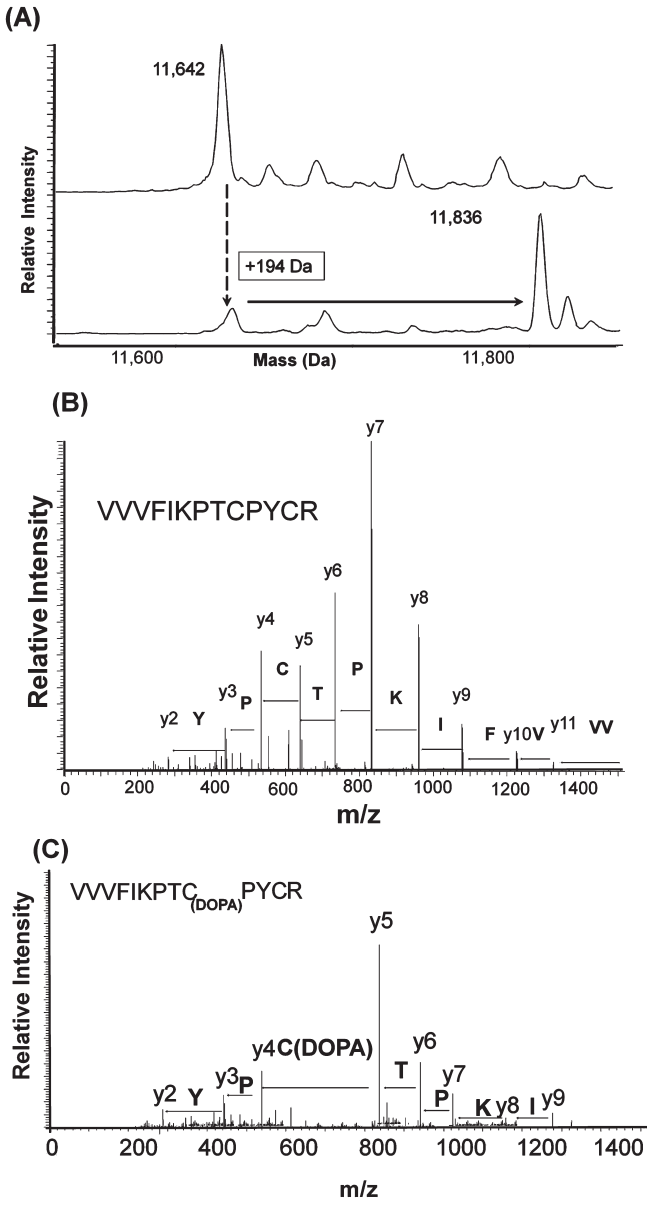

FIGURE 5: Quinone adduction occurs on the active-site Cys-22 of Grx. (A) Adduction of 194 Da was seen with the sample treated with oxidized L-DOPA (bottom) compared to the untreated sample (top). (B) MS/MS spectrum of untreated Grx. Fragmentation shows complete coverage of the active site. (C) MS/MS spectrum of L-DOPA-treated Grx. Fragmentation shows adduction of an ion at m/z 194 to Cys-22 within the active site.

GSH-deficient SHSY5Y cells (this study) overlaps the range of concentrations (*28*) in PD patients whose neurons are not only deficient in GSH but also impaired in mitochondrial function. We discovered that L-DOPA treatment leads to a loss of activity of the Grx and Trx systems in the neurons. Grx deactivation by L-DOPA was dose-dependent, and it was potentiated in GSH-depleted cells. Moreover, Grx inactivation occurred without a change in Grx content (Figure 2). TR and Trx activities were diminished after L-DOPA treatment of the SHSY5Y neurons with replete GSH in proportion to the loss of their respective contents (Figure 3). In cells with depleted GSH, however, TR was inhibited by L-DOPA, but its content was unchanged. The following considerations address the different modes of inactivation of the Grx and Trx systems.

Grx System. In previous studies, our research group learned that the cyclic disulfide-containing fungal toxin sporidesmon inactivates Grx by covalent modification of its active site, but sporidesmon has no effect on the other thiol disulfide oxidoreductases, GR, TR, or Trx (*29*). Our observation of inhibition of Grx in L-DOPA-treated cells with no change in its cellular content led us to predict a mechanism of inactivation analogous to sporidesmon adduction, involving covalent modification of Cys-22. Indeed, preincubation of Grx with oxidized L-DOPA gave concentration- and time-dependent decreases in activity which followed pseudo-first-order kinetics indicative of irreversible inactivation (Figure 4A,B). Unlike Grx, GR was not inactivated appreciably by oxidized L-DOPA (Figure 4C), consistent with retention of its activity in SHSY5Y cells treated with L-DOPA (Figure 3A).

The thiol moiety of Cys22 at the active site of Grx1 has an uncharacteristically low pK_a of 3.5 because of its local environment (*12*, *25*, *30*), making it much more reactive with thiol-modifying agents. GSH and typical protein cysteine residues have thiol pK_a values around 9, so their thiol groups remain protonated and less nucleophilic at physiological pH. The nucleophilic reactivity of the Grx active-site thiolate likely accounts for the selective inactivation of Grx via Michael addition of quinone, i.e., oxidized L-DOPA. Consistent with these interpretations, mass spectrometric results (Figure 5) document dopaquinone adduction of Grx on Cys-22. Although a recent proteomic study of isolated rat mitochondria treated with [^{14}C]dopamine revealed other proteins that contain radiolabel indicative of adduction (*31*), functional consequences were not examined, so it is unknown whether their modification might also contribute to cytotoxicity. Furthermore, knockdown of Grx by ~50% using siRNA (Figure 6) led to an increased level of apoptosis consistent with a requirement for Grx to maintain cell viability.

Implications of Grx Inactivation. Grx is implicated in the regulation of multiple cell signaling pathways that mediate apoptosis, cell growth, and cell survival (*32*−*36*). Hence, alterations in its deglutathionylase activity result in detrimental outcomes in many disease models (*25*). In particular, studies with Parkinson's disease show Grx1 is important for the maintenance of the mitochondrial permeability transition (*37*) and protection from MPTP-induced mitochondrial dysfunction (*38*). With inactivation of Grx by dopaquinone adduction (shown here), the neuronal cells lose the protective mechanism of deglutathionylation, and apoptotic cell death ensues.

Trx System. The Trx system is responsible for reduction of intra- and intermolecular disulfides and sulfenic acids (Scheme 1). Isolated Trx was not inactivated by oxidized L-DOPA (Figure 4C). Consistent with this result, Trx activity was unaffected also in cells where GSH was depleted and low concentrations of L-DOPA led to apoptosis. At higher concentrations of L-DOPA in cells with replete GSH, dose-dependent loss of Trx activity was observed (Figure 3). The latter result may reflect glutathionylation of the Trx protein on Cys residues separate from the active site, as reported previously (*39*), which could target it for degradation. Overall, the current observations, however, dissociate changes in Trx activity from the observed pattern of changes in L-DOPA-induced apoptosis.

Unlike the results for Trx, TR exhibits two different patterns of loss of activity in cells treated with L-DOPA depending on the GSH status, perhaps reflecting different modes of regulation of its activity under different redox conditions. TR shows a parallel decrease in content and activity in response to L-DOPA treatment in neurons with replete GSH, similar to Trx. This observation is consistent with the lack of adductive deactivation of the isolated

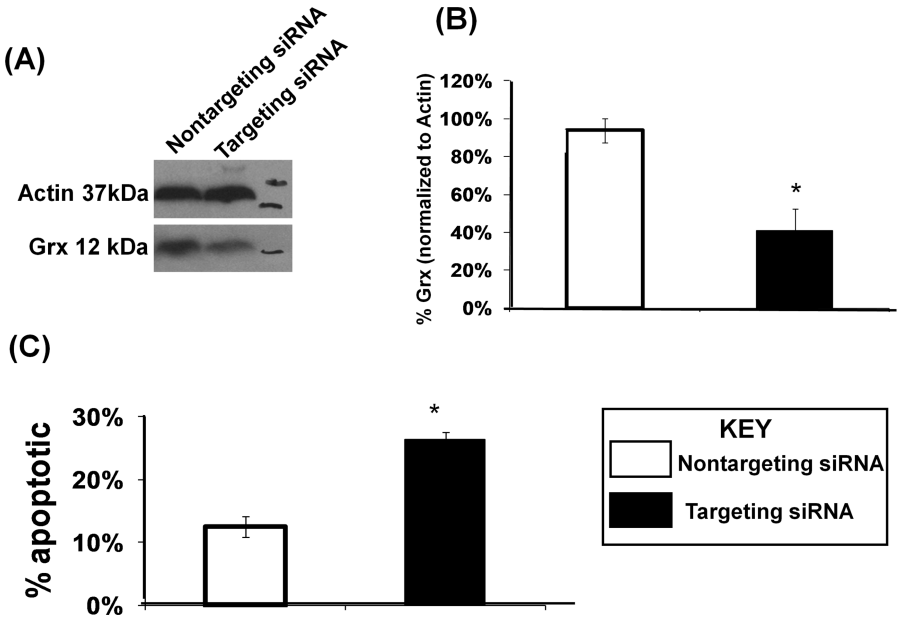

FIGURE 6: Knockdown of Grx results in an increased level of apoptosis in SHSY5Y cells. (A) Typical Western blot confirming Grx1 knockdown relative to controls and compared to actin (loading control). (B) Bar graph showing densitometric quantification of Grx1 knockdown. (C) Bar graph showing relative apoptosis for control SHSY5Y cells vs cells in which Grx1 was knocked down (Grx1-siRNA). Apoptosis was assessed in triplicate by chromatin condensation in a blinded fashion using Hoechst 33342 dye. An asterisk indicates $p < 0.01$ ($n = 3$ independent biological samples).

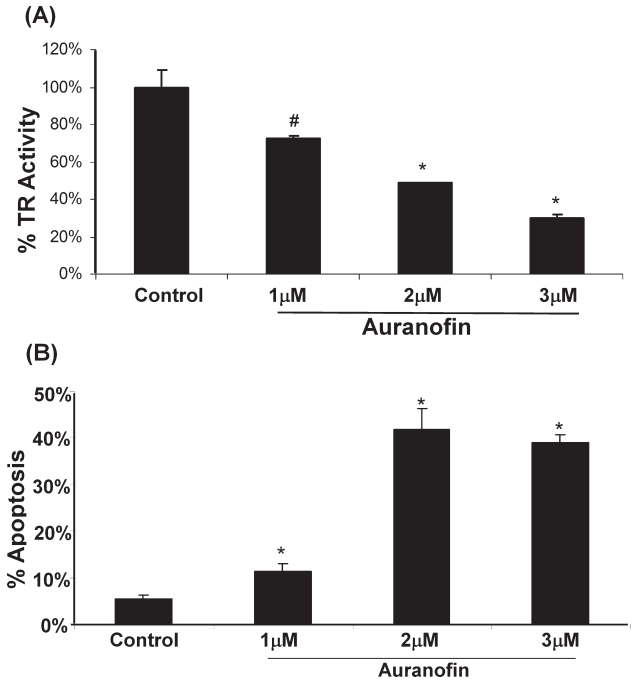

FIGURE 7: Inhibition of TR increases the level of apoptosis in SHSY5Y cells. (A) Bar graph showing the auranofin concentration-dependent increase in the level of apoptosis of SHSY5Y cells. Apoptosis was measured 24 h after treatment according to chromatin condensation (Hoechst staining). Asterisks indicate $p < 0.01$ ($n = 3$); measurements were taken in triplicate. (B) Bar graph showing auranofin concentration-dependent inhibition of TR in SHSY5Y cells. Auranofin was titrated to give inhibition equal to that seen with L-DOPA treatment. A number sign indicates $p < 0.05$; an asterisk indicates $p < 0.01$ ($n = 3$).

TR enzyme by oxidized L-DOPA, since the remaining TR protein obtained from the cells was fully active. However, cotreatment with L-DOPA and BSO (depleting GSH) led to loss of TR activity with no change in its content (Figure 3). This result contrasts with the study of the isolated enzyme, where no inhibition was observed (Figure 4) after preincubation with concentrations of oxidized L-DOPA that certainly exceed what would be generated in the SHSY5Y cells and what would occur in PD patients.

Several alternative considerations might explain the paradoxical data for TR. In the case where the decrease in TR activity corresponds to a decrease in content, this suggests that a modification of the TR targets it for degradation under conditions of replete GSH. For example, glutathionylation of TR is a likely oxidative modification under L-DOPA-induced oxidative stress when GSH is abundant and deglutathionylation by Grx is deactivated. In cells with depleted GSH glutathionylation becomes less likely, so that irreversible oxidation at the TR active site such as formation of sulfinic and sulfonic acids may result in loss of activity without a signal for protease degradation.

Alternatively, TR may be inhibited by metal ion release in response to L-DOPA treatment. Indeed, treatment with 6-OHDA leads to the release of iron (Fe^{2+} and Fe^{3+}) from stores, which may contribute to ROS generation and oxidant-induced cell death (*40*, *41*). With the absence of GSH, iron ions have a weakened ability to be chelated and thus can bind to the TR active-site thiols, resulting in inhibition without concomitant degradation.

Regardless of the specific mechanism, loss of TR activity may compromise cell viability. Consistent with this interpretation, inhibition of TR by auranofin increased the level of cell death (Figure 7).

Cellular Implications for Inhibition of the Trx System. TR is required for maintenance of the Trx system which reduces intra- and intermolecular disulfide bonds, and Trx has been observed in a number of studies to be neuroprotective, including cell culture studies showing protection from MPP+ treatment (*42*). Loss of TR not only impedes reduction of certain oxidative thiol modifications but also activates cell signaling pathways that mediate cell death (*43*). Thus, inhibition of either the Trx or Grx system or both leads to increased levels of

SHSY5Y neuronal cell death. Comparison of the effects on apoptosis of ~50% inhibition of TR by auranofin or ~50% knockdown of Grx to the effects of L-DOPA treatment suggests that impairment of the two enzyme systems contributes in an additive fashion to L-DOPA-induced apoptosis (Figures 1C, 2C, 3A, 6, and 7).

CONCLUSIONS

L-DOPA treatment of neuronal cells induces cell death in a concentration-dependent fashion that is potentiated in GSH-deficient cells. L-DOPA leads to inactivation of Grx both in isolation and in neuronal cells. This inactivation appears to occur through irreversible quinone adduction of the enzyme active site. Furthermore, L-DOPA decreases TR and Trx content which adds to the overall disruption of sulfhydryl homeostasis. The net result is an increased level of apoptotic death of the SHSY5Y neurons. Both the Grx and Trx systems have been implicated in regulation of key intermediates in apoptotic signaling cascades, so inhibition of either or both of these enzyme systems impedes cell survival.

Further studies to delineate how each of these two enzyme systems alters specific cell signaling mechanisms leading to an increased level of neuronal cell death would be beneficial in devising approaches to counteract the potential adverse affects of L-DOPA treatment in PD patients.

ACKNOWLEDGMENT

We appreciate the technical assistance of Mary Consolo, who prepared the [^{3}H]BSA-SSG substrate and purified Grx. We are grateful to Dr. Joseph Liedhegner (Johnson Controls Inc., Milwaukee, WI) for assistance in data analysis, and we thank Dr. Ruth Siegel (Case Western Reserve University Department of Pharmacology) for critical review of the manuscript.

REFERENCES

1. Riedlerer, P. F. (2004) Views on neurodegeneration as a basis for neuroprotective strategies. *Med. Sci. Monit. 10*, RA287–RA290.
2. Maguire-Zeiss, K. A., Short, D. W., and Federoff, H. J. (2005) Synuclein, dopamine and oxidative stress: Co-conspirators in Parkinson's disease? *Brain Res. Mol. Brain Res. 134*, 18–23.
3. Olanow, C. W., and Tatton, W. G. (1999) Etiology and pathogenesis of Parkinson's disease. *Annu. Rev. Neurosci. 22*, 123–144.
4. Walkinshaw, G., and Waters, C. M. (1995) Induction of apoptosis in catecholaminergic PC12 cells by L-DOPA. Implications for the treatment of Parkinson's disease. *J. Clin. Invest. 95*, 2458–2464.
5. Asanuma, M., Miyazaki, I., az-Corrales, F. J., and Ogawa, N. (2004) Quinone formation as dopaminergic neuron-specific oxidative stress in the pathogenesis of sporadic Parkinson's disease and neurotoxin-induced parkinsonism. *Acta Med. Okayama 58*, 221–233.
6. Spencer, J. P., Jenner, A., Butler, J., Aruoma, O. I., Dexter, D. T., Jenner, P., and Halliwell, B. (1996) Evaluation of the pro-oxidant and antioxidant actions of L-DOPA and dopamine in vitro: Implications for Parkinson's disease. *Free Radical Res. 24*, 95–105.
7. Ahlskog, J. E. (2007) Beating a dead horse: Dopamine and Parkinson disease. *Neurology 69*, 1701–1711.
8. Legros, H., Dingeval, M. G., Janin, F., Costentin, J., and Bonnet, J. J. (2004) Toxicity of a treatment associating dopamine and disulfiram for catecholaminergic neuroblastoma SH-SY5Y cells: Relationships with 3,4-dihydroxyphenylacetaldehyde formation. *Neurotoxicology 25*, 365–375.
9. Klegeris, A., and McGeer, P. L. (2000) R-(−)-Deprenyl inhibits monocytic THP-1 cell neurotoxicity independently of monoamine oxidase inhibition. *Exp. Neurol. 166*, 458–464.
10. Chrestensen, C. A., Eckman, C. B., Starke, D. W., and Mieyal, J. J. (1995) Cloning, expression and characterization of human thioltransferase (glutaredoxin) in *E. coli* 1. *FEBS Lett. 374*, 25–28.
11. Chrestensen, C. A., Starke, D. W., and Mieyal, J. J. (2000) Acute cadmium exposure inactivates thioltransferase (glutaredoxin), inhibits intracellular reduction of protein-glutathionyl-mixed disulfides, and initiates apoptosis. *J. Biol. Chem. 275*, 26556–26565.
12. Jao, S. C., English Ospina, S. M., Berdis, A. J., Starke, D. W., Post, C. B., and Mieyal, J. J. (2006) Computational and mutational analysis of human glutaredoxin (thioltransferase): Probing the molecular basis of the low pKa of cysteine 22 and its role in catalysis. *Biochemistry 45*, 4785–4796.
13. Gallogly, M. M., Starke, D. W., Leonberg, A. K., English Ospina, S. M., Gillenberger, S., and Mieyal, J. J. (2007) Correspondence of the Catalytic Mechanisms of the Mammalian Glutaredoxin 1 and Glutaredoxin 2 Enzymes: Functional Implications.
14. Starke, D. W., Chen, Y., Bapna, C. P., Lesnefsky, E. J., and Mieyal, J. J. (1997) Sensitivity of protein sulfhydryl repair enzymes to oxidative stress. *Free Radical Biol. Med. 23*, 373–384.
15. Carlberg, I., and Mannervik, B. (1985) Glutathione reductase. *Methods Enzymol. 113*, 484–490.
16. Arner, E. S., Zhong, L., and Holmgren, A. (1999) Preparation and assay of mammalian thioredoxin and thioredoxin reductase. *Methods Enzymol. 300*, 226–239.
17. Gravina, S. A. (1993) Characterization and Kinetic Mechanism of Thioltransferase, Ph.D. Thesis, Case Western Reserve University, Cleveland, OH.
18. Perry, T. L., Godin, D. V., and Hansen, S. (1982) Parkinson's disease: A disorder due to nigral glutathione deficiency? *Neurosci. Lett. 33*, 305–310.
19. Jenner, P., Dexter, D. T., Sian, J., Schapira, A. H., and Marsden, C. D. (1992) Oxidative stress as a cause of nigral cell death in Parkinson's disease and incidental Lewy body disease. The Royal Kings and Queens Parkinson's Disease Research Group. *Ann. Neurol. 32* (Suppl.), S82–S87.
20. Sian, J., Dexter, D. T., Lees, A. J., Daniel, S., Agid, Y., Javoy-Agid, F., Jenner, P., and Marsden, C. D. (1994) Alterations in glutathione levels in Parkinson's disease and other neurodegenerative disorders affecting basal ganglia. *Ann. Neurol. 36*, 348–355.
21. Ziegler, D. M. (1985) Role of reversible oxidation-reduction of enzyme thiols-disulfides in metabolic regulation. *Annu. Rev. Biochem. 54*, 305–329.
22. Mieyal, J. J., Srinivasan, U., Starke, D. W., Gravina, S. A., and Mieyal, P. A. (1995) in Glutathionyl Specificity of the Thioltransferases: Mechanistic and Physiological Implications (Packer, L., and Cadenas, E., Eds.) pp 305−372, Marcel Dekker, Inc., New York.
23. Sabens, E. A., and Mieyal, J. J. (2009) Glutaredoxin and Thioredoxin Enzyme Systems: Catalytic Mechanisms and Physiological Functions. In Glutathione and Sulfer Amino Acids in Human Health and Disease (Masella, R., and Mazza, G., Eds.) pp 121−156, John Wiley and Sons, Inc., Hoboken, NJ.
24. Jacob, C., Knight, I., and Winyard, P. G. (2006) Aspects of the biological redox chemistry of cysteine: From simple redox responses to sophisticated signalling pathways. *Biol. Chem. 387*, 1385–1397.
25. Mieyal, J. J., Gallogly, M. M., Qanungo, S., Sabens, E. A., and Shelton, M. D. (2008) Molecular mechanisms and clinical implications of reversible protein S-glutathionylation. *Antioxid. Redox Signaling 10*, 1941–1988.
26. Cox, A. G., Brown, K. K., Arner, E. S., and Hampton, M. B. (2008) The thioredoxin reductase inhibitor auranofin triggers apoptosis through a Bax/Bak-dependent process that involves peroxiredoxin 3 oxidation. *Biochem. Pharmacol. 76*, 1097–1109.
27. Gandin, V., Fernandes, A. P., Rigobello, M. P., Dani, B., Sorrentino, F., Tisato, F., Bjornstedt, M., Bindoli, A., Sturaro, A., Rella, R., and Marzano, C. (2010) Cancer cell death induced by phosphine gold(I) compounds targeting thioredoxin reductase. *Biochem. Pharmacol. 79*, 90–101.
28. Brunton, L., Lazo, J., and Parker, K. (2010) The Pharmacological Basis of Therapeutics, McGraw Hill, New York.
29. Srinivasan, U., Bala, A., Jao, S. C., Starke, D. W., Jordan, T. W., and Mieyal, J. J. (2006) Selective inactivation of glutaredoxin by sporidesmin and other epidithiopiperazinediones. *Biochemistry 45*, 8978–8987.
30. Srinivasan, U., Mieyal, P. A., and Mieyal, J. J. (1997) pH profiles indicative of rate-limiting nucleophilic displacement in thioltransferase catalysis. *Biochemistry 36*, 3199–3206.
31. Van, L. V., Mishizen, A. J., Cascio, M., and Hastings, T. G. (2009) Proteomic identification of dopamine-conjugated proteins from isolated rat brain mitochondria and SH-SY5Y cells. *Neurobiol. Dis. 34*, 487–500.
32. Klatt, P., Molina, E. P., De Lacoba, M. G., Padilla, C. A., Martinez-Galesteo, E., Barcena, J. A., and Lamas, S. (1999) Redox regulation of c-Jun DNA binding by reversible S-glutathiolation. *FASEB J. 13*, 1481–1490.

33. Wang, J., Tekle, E., Oubrahim, H., Mieyal, J. J., Stadtman, E. R., and Chock, P. B. (2003) Stable and controllable RNA interference: Investigating the physiological function of glutathionylated actin. *Proc. Natl. Acad. Sci. U.S.A. 100*, 5103–5106.
34. Klatt, P., Molina, E. P., and Lamas, S. (1999) Nitric oxide inhibits c-Jun DNA binding by specifically targeted S-glutathionylation. *J. Biol. Chem. 274*, 15857–15864.
35. Wang, J., Boja, E. S., Tan, W., Tekle, E., Fales, H. M., English, S., Mieyal, J. J., and Chock, P. B. (2001) Reversible glutathionylation regulates actin polymerization in A431 cells. *J. Biol. Chem. 276*, 47763–47766.
36. Qanungo, S., Starke, D. W., Pai, H. V., Mieyal, J. J., and Nieminen, A. L. (2007) Glutathione supplementation potentiates hypoxic apoptosis by S-glutathionylation of p65-NFκB. *J. Biol. Chem. 282*, 18427–18436.
37. Saeed, U., Durgadoss, L., Valli, R. K., Joshi, D. C., Joshi, P. G., and Ravindranath, V. (2008) Knockdown of cytosolic glutaredoxin 1 leads to loss of mitochondrial membrane potential: Implication in neurodegenerative diseases. *PLoS One 3*, e2459.
38. Kenchappa, R. S., Diwakar, L., Annepu, J., and Ravindranath, V. (2004) Estrogen and neuroprotection: Higher constitutive expression of glutaredoxin in female mice offers protection against MPTP-mediated neurodegeneration. *FASEB J. 18*, 1102–1104.
39. Casagrande, S., Bonetto, V., Fratelli, M., Gianazza, E., Eberini, I., Massignan, T., Salmona, M., Chang, G., Holmgren, A., and Ghezzi, P. (2002) Glutathionylation of human thioredoxin: A possible cross-talk between the glutathione and thioredoxin systems. *Proc. Natl. Acad. Sci. U.S.A. 99*, 9745–9749.
40. Wang, J., Jiang, H., and Xie, J. X. (2004) Time dependent effects of 6-OHDA lesions on iron level and neuronal loss in rat nigrostriatal system. *Neurochem. Res. 29*, 2239–2243.
41. Borisenko, G. G., Kagan, V. E., Hsia, C. J., and Schor, N. F. (2000) Interaction between 6-hydroxydopamine and transferrin: "Let my iron go". *Biochemistry 39*, 3392–3400.
42. Masutani, H., Bai, J., Kim, Y. C., and Yodoi, J. (2004) Thioredoxin as a neurotrophic cofactor and an important regulator of neuroprotection. *Mol. Neurobiol. 29*, 229–242.
43. Rundlof, A. K., and Arner, E. S. (2004) Regulation of the mammalian selenoprotein thioredoxin reductase 1 in relation to cellular phenotype, growth, and signaling events. *Antioxid. Redox Signaling 6*, 41–52.